AIP | Review of Scientific Instruments

A self-adjustable four-point probing system using polymeric three dimensional coils and non-toxic liquid metal

Nomin-Erdene Oyunbaatar, Yong Soo Choi, and Dong-Weon Lee

Citation: Review of Scientific Instruments **86**, 125006 (2015); doi: 10.1063/1.4938252
View online: http://dx.doi.org/10.1063/1.4938252
View Table of Contents: http://scitation.aip.org/content/aip/journal/rsi/86/12?ver=pdfcov
Published by the AIP Publishing

A self-adjustable four-point probing system using polymeric three dimensional coils and non-toxic liquid metal

Nomin-Erdene Oyunbaatar, Yong Soo Choi, and Dong-Weon Lee[a)]
MEMS and Nanotechnology Laboratory, School of Mechanical Engineering, Chonnam National University, Gwangju 500757, South Korea

(Received 2 July 2015; accepted 8 December 2015; published online 28 December 2015)

This paper describes a self-adjustable four-point probe (S4PP) system with a square configuration. The S4PP system consists of 3D polymer coil springs for the independent operation of each tungsten (W) probe, microfluidic channels filled with a nontoxic liquid metal, and a LabView-based control system. The 3D coil springs made by PMMA are fabricated with a 3D printer and are positioned in a small container filled with the non-toxic liquid metal. This unique configuration allows independent self-adjustment of the probe heights for precise measurements of the electrical properties of both flexible and large-step-height microsamples. The feasibility of the fabricated S4PP system is evaluated by measuring the specific resistance of Cr and Au thin films deposited on silicon wafers. The system is then employed to evaluate the electrical properties of a Au thin film deposited onto a flexible and easily breakable silicon diaphragm (spring constant: $\sim 3.6 \times 10^{-5}$ N/m). The resistance of the Cr thin films (thickness: 450 nm) with step heights of 60 and 90 μm is also successfully characterized. These experimental results indicate that the proposed S4PP system can be applied to common metals and semiconductors as well as flexible and large-step-height samples. © *2015 AIP Publishing LLC.* [http://dx.doi.org/10.1063/1.4938252]

I. INTRODUCTION

Over the past 20 years, various technologies such as eddy-current, microwave, two-point probe (2PP), and four-point probe (4PP) systems have been introduced in order to analyze the electrical properties of metals and semiconductors.[1–8] Among them, the 4PP method is widely used in various fields because the contact resistance between the sample and the probe can be ignored during the measurement.[9] The 4PP method can be divided into two types with square and linear configurations. The 4PP with a linear configuration (L4PP) employs four serial probes with an interval of several mm. It is frequently utilized to measure the specific resistance and sheet resistance of metal thin films formed on the surfaces of semiconductors and insulators. In contrast, the 4PP with a square configuration (S4PP) can measure the electron concentration of a semiconductor by using the Hall effect and also characterize the anisotropic electrical properties of crystalline materials such as silicon.[10] Although the 4PP is a standard method for studying the electrical properties of solids and thin films, it still needs to be improved for further applications. For example, the commercially available 4PP cannot be used on the surfaces of samples with a large step height or those that are made of flexible and easily breakable materials because of the operating distance limitations of the probe and the rigidity of its spring. In an effort to overcome this drawback, Ju *et al.* proposed a flexible 4PP with a spring constant of 6 pN/nm that uses microelectromechanical systems (MEMS) technology and evaluated the electrical properties of various materials by mounting the fabricated device on an atomic force microscope (AFM).[11] Petersen *et al.* presented a flexible 4PP based on a scanning tunneling microscope (STM), but their probe is only able to function as a spring with a small displacement because of its small body.[12] Keller *et al.* fabricated a micro-4PP with SU-8 photoresist to reduce the contact force between the probe and the sample and measured the specific resistance of a thin metal layer with their proposed device.[13] However, most of these proposed methods are limited to small-step-height samples and utilize expensive AFMs and STMs to measure the sample resistance.

In this study, a low-cost S4PP integrated with a polymer spring was designed and fabricated to measure the specific resistance of samples that are flexible as well as have large step heights. The proposed S4PP consists of sharp W probes with a high-aspect ratio, polymer springs fabricated using a ProJet HD 3500 Plus Professional 3D printer (3D Systems Corp., USA), a 4PP body with microfluidic channels, and a conductive liquid metal (3.46×10^6 S/m) for electrical connections. The polymer springs are positioned in a small container filled with the nontoxic liquid metal to improve their flexibility and buffering effect. After basic experiments, the specific resistance of a metal thin film formed onto a thin silicon diaphragm was successfully characterized using the fabricated S4PP system.

II. DESIGN AND FABRICATION

A. Four-point probe with a square configuration

The S4PP measurement system was effectively used to evaluate the electrical properties of various materials.[14,15] Conventional commercial 4PP and micro-4PP are difficult for large-step-height samples owing to the operating limits of

a)Author to whom correspondence should be addressed. Electronic mail: mems@jnu.ac.kr. Tel.: +82 62 530 1684. Fax: +82 62 530 1689.

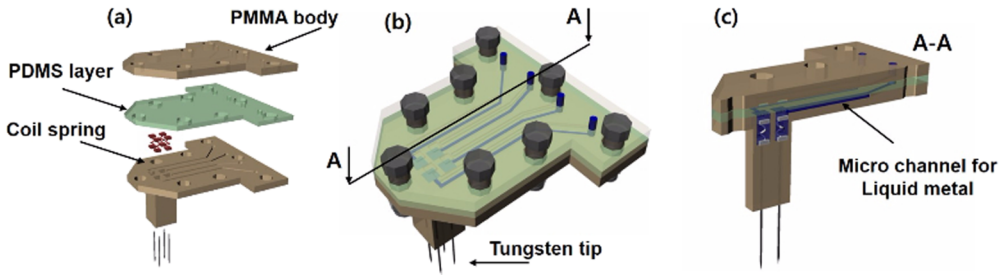

FIG. 1. (a) Schematic of (a) components for the square-configured 4PP (S4PP) and (b) the assembled S4PP system. (c) A cross-sectional view of the proposed S4PP.

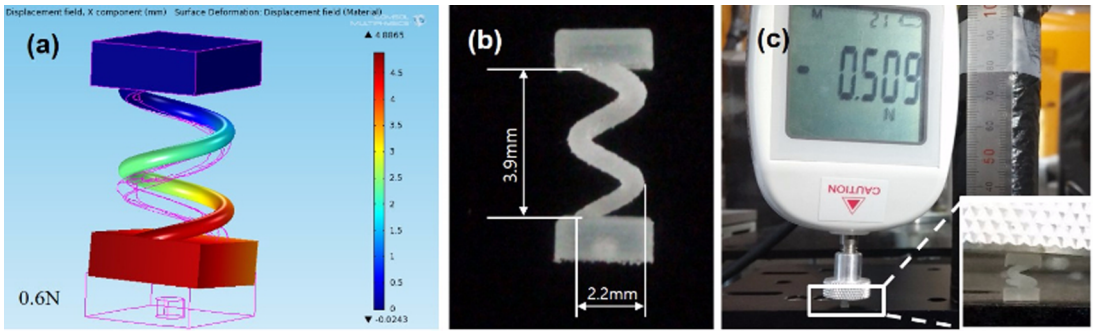

FIG. 2. (a) FEM analysis of the 3D polymer coil spring, (b) an optical image of the fabricated 3D coil spring, and (c) displacement of the 3D coil spring as a function of a force.

their probes. Figs. 1(a)-1(c) show a schematic of the proposed S4PP and its cross section. The polymer spring helps the W probe make flexible contact with a sample surface. W tips with a high-aspect ratio were electrically connected to an external system through the liquid metal filled in microfluidic channels. The width and depth of each liquid metal channel were designed as 800 μm to ensure easy injection of the liquid metal into the microchannels. To avoid any leakage of liquid metal from the microchannel, a polydimethylsiloxane (PDMS) layer was inserted between the bottom and the cover PMMA plates. The four microchannels filled with liquid metal were designed to be independently connected to each W probe. As shown in Figs. 2(a) and 2(b), a square groove formed on the lower part of the PMMA coil which helps the alignment of the tungsten probe (diameter: 300 μm) to be positioned at the middle of the spring.

To optimize the structure and spring constant of the polymer coil spring, the displacement of the spring as a function of applied force was analyzed by using the commercial program COMSOL as shown in Fig. 2(a). A 3D model of the polymer coil was designed by using the CATIA program, and an analysis was carried out by importing this model into the COMSOL program. The material properties of the PMMA used to simulate the spring constant are as follows: a Young's modulus of 2 GPa, a density of 1.18 g/cm^3, and a Poisson ratio of 0.3. Finally, the diameter and length of the PMMA spring were fixed at 2.2 and 3.9 mm, respectively. The calculated spring constant of the PMMA coil was approximately 140 N/m. The designed 3D coil springs were fabricated to a specific size on the basis of the analysis results. An optical image of the fabricated coil spring is shown in Fig. 2(b). The spring constant was also experimentally confirmed using a pull-push force gauge (China, HF-5 Model) as shown in Fig. 2(c). Figure 3 compares the analysis and experimental results for the probe displacement for various forces applied to the PMMA coil spring. The analysis and experimental results were quite close and within an error range of 10%. From the experimental results, we found that the coil spring was gradually compressed until the applied force reached about 0.7 N. At a force of 0.8 N or higher, the displacement became consistent at 3.6 mm. This range can be varied by employing different types of the 3D coil.

The fabricated polymer coil springs were placed in a small container filled with the nontoxic liquid metal, which helps the tungsten probe make flexible contact with a fragile

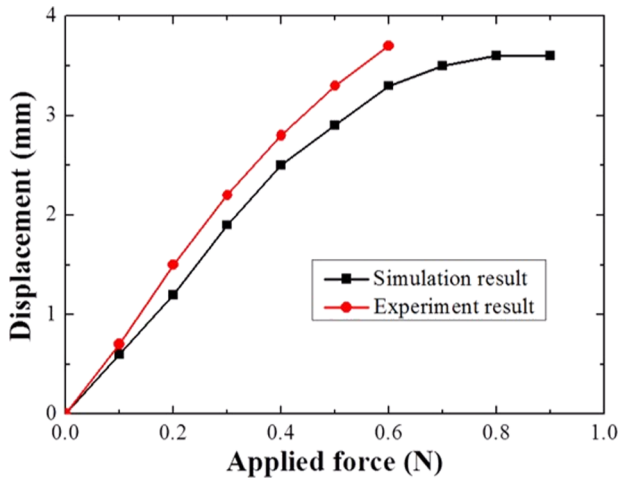

FIG. 3. Comparison of the analysis and experimental results for the coil spring displacement.

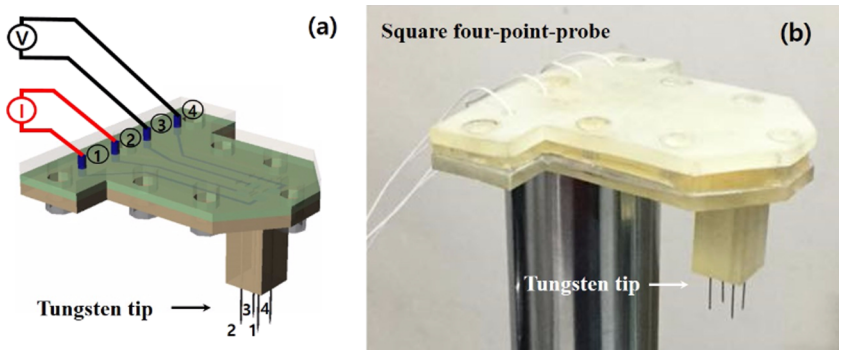

FIG. 4. (a) Configuration of the S4PP for the probe arrangement and (b) an optical image of the fabricated S4PP.

sample. The operating range of the fabricated coil springs was limited to a maximum distance of 3.5 mm. Passing a current through two W probes (Nos. 1 and 2) and measuring the voltage drop through other two W probes (Nos. 3 and 4) allow the measurement of the substrate resistivity. Figs. 4(a) and 4(b) show the method for measuring the specific resistance with the 4PP having a square arrangement and a photograph of the fabricated S4PP.

B. Tungsten-tip preparation

The electrolytic etching method[16] is widely employed to fabricate a high-aspect W-tip easily and quickly in air.[17] There are several efficient methods to fabricate very long and conical-shaped W-tips suitable for nanometer scale probing. Hobara *et al.* proposed a reliable method by the use of a dynamic electrochemical method and a drop-off method.[18] The cone angle of the W-tips can be controlled by changing the speed of tip pulling-up from the electrolyte solution. Park *et al.* also developed a self-descending phenomenon of menisci for a high aspect ratio W-tip with a stepped shape.[19] In this experiment, we have used the stepped W-tip fabrication method by adjusting the proper distance of the counter electrode considering reproducibility of the W-tip. Surface meniscus at the cathode and the wall can produce unique high-quality W tip. Briefly, 8 g of NaOH was placed into 100 ml of DI water in a glass beaker, and an etching solution was prepared by using an ultrasonicator for 10 min. The etching solution was poured into a homemade Teflon bath, and 0.3-mm-thick W wires were dipped into the etching solution to a depth of 5 mm. Next, a voltage of 4 V was applied between two W wires by using a DC power supply. This resulted in the W wires being selectively etched by the electrolyte solution. The etching time for fabrication of sharp W probes was controlled by the current. As shown in Fig. 5(a), the end of the probe automatically separated from the etching solution when the fabrication of a W probe was complete, and the flow of electric current immediately stopped without any help of a control unit. This is due to the use of the home-made Teflon bath instead of a conventional glass beaker. The hydrophobic surface of a wall in the Teflon bath and properly positioned Pt wire (counter electrode) provide a unique characteristic during the W tip fabrication. Figs. 5(b) and 5(c) show optical and SEM images of a W probe fabricated via the conventional electrolytic etching method. Fig. 5(d) shows the SEM image of a W probe fabricated using

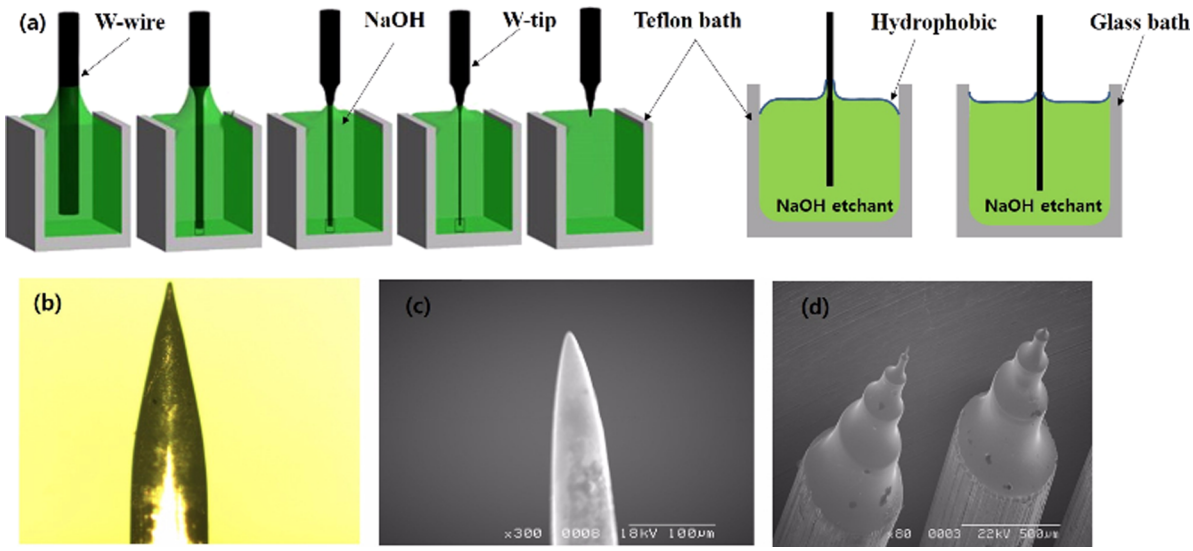

FIG. 5. (a) A process flow for the fabrication of a tungsten tip with a unique shape, (b) optical microscope image, and (c) SEM image of the fabricated W probes using a conventional method. (d) SEM images of the fabricated W probes using the Teflon bath with the hydrophobic characteristics.

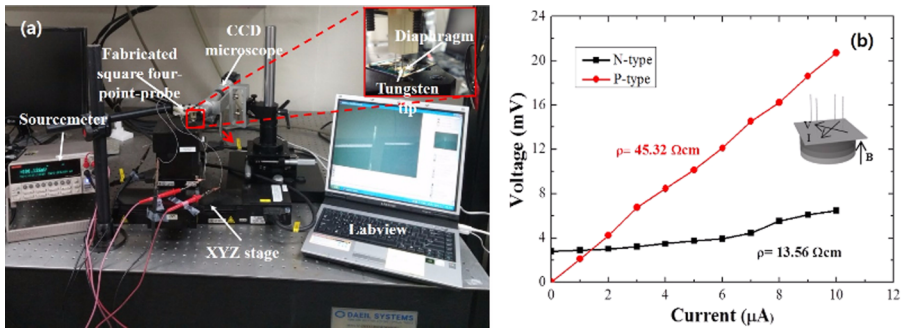

FIG. 6. (a) Experimental setup for the characterization of semiconductors using the fabricated S4PP and (b) current-voltage characteristics of n-type and p-type semiconductors.

the home-made Teflon bath. The fabricated W probe had a high aspect ratio and sharp tip. An additional coating of Au or Pt improves the electrical conductivity and prevents the oxidation of the W probe.

III. MEASUREMENT THEORY AND EXPERIMENTAL RESULTS

The electrical properties of samples can be evaluated by applying a constant current to two W probes positioned either in parallel or diagonally and by measuring the voltage drop that occurs between the remaining two W probes. When the two probes are positioned in parallel, the resistivity ρ of the samples can be analyzed without any influence of contact resistance between the sample and the W probe. When the two probes are positioned diagonally, the Hall voltage can be analyzed due to the unique configuration of the probes. Additionally, the Hall coefficient, carrier concentration of semiconductors, and the conductivity type (n or p) are all derived from the Hall voltage measurement.[20]

Fig. 6(a) shows the measurement system constructed with the fabricated S4PP. The measurement system consisted of the S4PP head with four W probes, an XYZ motorized stage (M-ILS150CC, M-GTS30V, Newport) for precise control, a CCD-mounted high-resolution microscope for real-time observation of the contact condition, and a source meter (2410, Keithley) for applying a current and measuring the voltage between two W probes. All of the parts in the measurement system were linked to and controlled by the LabView software for fast and precise measurements.

When four W probes contact on the arbitrary shaped flat surface along the circumference, shown in Fig. 4(a), the resistivity of the materials is defined as $R_{12,34}$ or $R_{23,41}$,

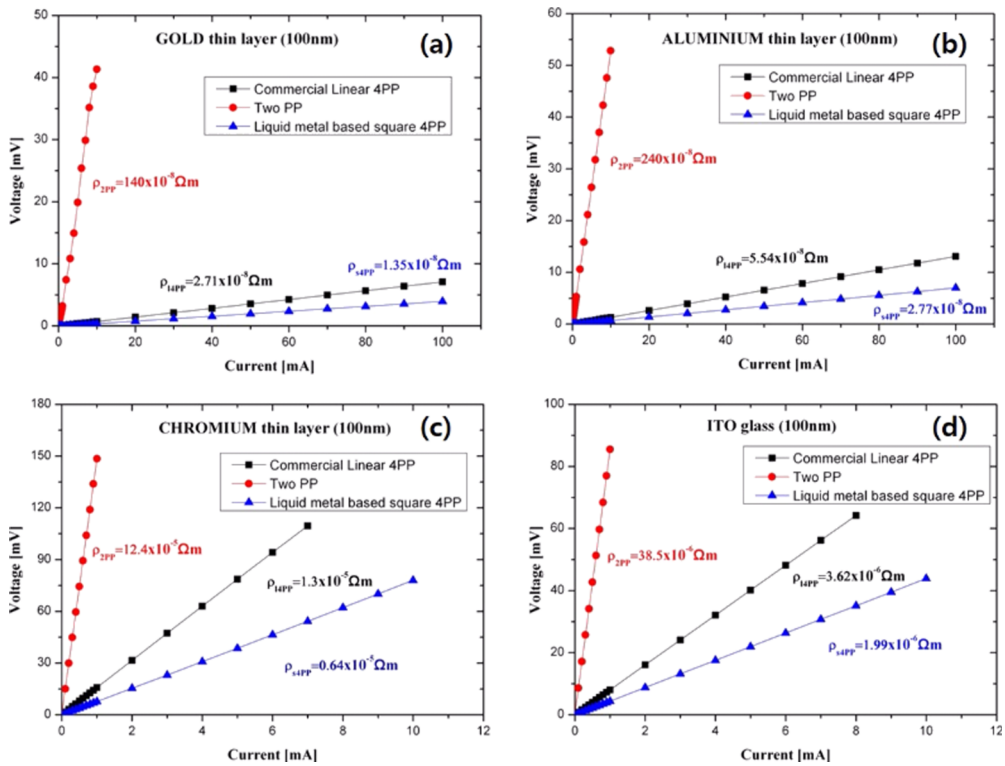

FIG. 7. Characterization of the electrical resistance for various materials such as (a) a Au thin film, (b) an Al thin film, (c) a Cr thin film, and (d) an ITO thin film.

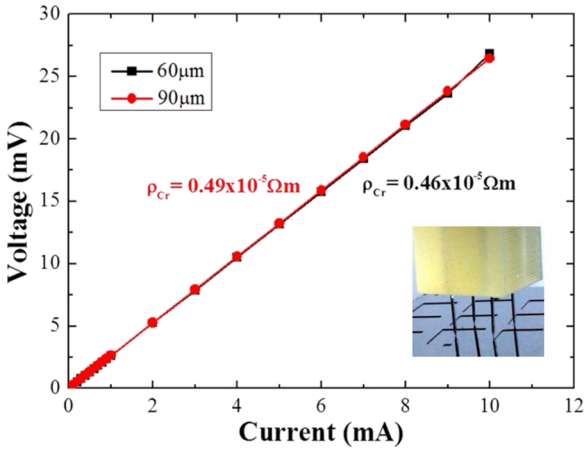

FIG. 8. Experimental results of the specific resistance for Cr-coated samples with 60 μm and 90 μm step heights.

respectively.[21] The relation between two resistances is shown in the following equation:

$$\exp(\pi R_{12,34}\, d/\rho) + \exp(\pi R_{23,41}\, d/\rho) = 1, \quad (1)$$

where ρ is specific resistance of the material and d is the thickness of a sample. Based on the equation, the specific resistance of a sample is defined in Equation (2),

$$\rho = \frac{\pi d}{\ln 2} \cdot \frac{R_{12,34} + R_{23,41}}{2} \cdot f\left(\frac{R_{12,34}}{R_{23,41}}\right), \quad (2)$$

where f is a function of the ratio $R_{12,34}/R_{23,41}$ and is only satisfied by the relation

$$\frac{R_{12,34} - R_{23,41}}{R_{12,34} + R_{23,41}} = f \cdot \arccos h\left(\frac{\exp(\ln 2/f)}{2}\right). \quad (3)$$

Basic experiments on the resistivity measurements were carried out using the fabricated S4PP system and silicon wafers. The input program displayed the specific resistance of silicon wafers in real-time, as shown in Fig. 6(b).

Fig. 7 shows the specific resistances measured for various samples (i.e., Au, Al, Cr, and ITO) deposited onto an insulator with a two-point-probe method, a commercial L4PP, and the proposed S4PP. To ensure the reproducibility of the measurement results, the specific resistance was measured three times for each sample. The metal thin film used in the measurement had a thickness of 100 nm. The proposed S4PP system operated independently to make contact with the metal thin film with the motorized stage, and the specific resistance of the sample was obtained by using the source meter. The experimental results showed that the accuracy of the measured values was different between two-point-probe and four-point-probe methods. This was caused by the problem of the contact resistance of the two-point-probe method.[22] However, the measured resistivity by the commercial 4PP was very close to that of the proposed S4PPs. A slight difference between two 4PP methods is due to the influence of a pitch distance on 4PP, thickness of samples, and material properties (conductors or insulators). Some researchers[23,24] also reported the difference of the two kinds of 4PP measurement systems. The resistivity of the material can be expressed as $\rho = (\Delta V/I)2\pi s$ and $\rho = (\Delta V/I)(2\pi s/2 - \sqrt{2})$ for linear- and square-configured-four-point probes, respectively. From our measurement results, it should be noted that the specific resistance of the metal thin layer belongs to the geometric conditions of four probes, not to the probe distance.

To confirm the self-height adjustment function of the fabricated S4PP, two different samples with step heights of 60 and 90 μm were prepared using a silicon wet-etching method. A Cr thin film with a thickness of 450 nm was coated on the sample surface. The specific resistance of Cr for each sample was measured three times in succession to confirm the measurement reproducibility. Fig. 8 shows the measured resistivity of Cr thin films coated on 60 and 90 μm step heights. The specific resistances measured for each sample were clearly consistent and virtually the same as the specific resistance values measured using the S4PP in Fig. 7. These experimental results showed that the proposed S4PP can be applied to samples with large step heights, which cannot be measured with the conventional L4PP.

To confirm the usability of the fabricated S4PP on flexible materials, the specific resistance of a silicon diaphragm coated with Au with a thickness of 14 μm (spring constant: approximately 3.6×10^{-5} N/m) was measured. The diaphragm structure was fabricated by using a conventional micromachining process, and a 100-nm-thick Au film was deposited onto the silicon diaphragm by using e-beam evaporation. Figs. 9(a) and 9(b) show optical images of the probes making contact with a sample surface to measure the specific resistance of the Au thin film deposited onto the silicon diaphragm using the commercial L4PP and the fabricated S4PP, respectively. When the commercial L4PP made contact with the Au thin film deposited onto the

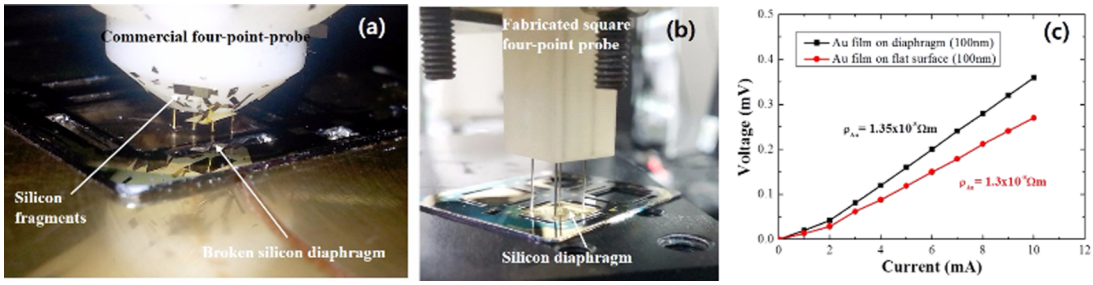

FIG. 9. Optical images of (a) a commercial L4PP and (b) the fabricated S4PP contacted onto a thin silicon diaphragm with a spring constant of about 3.6×10^{-5} N/m. (c) Specific resistance of a 100-nm-thick Au film deposited on the silicon diaphragm using the S4PP.

silicon diaphragm, it was impossible to measure the specific resistance because the Si diaphragm was fractured. On the other hand, the proposed S4PP with a polymer spring was possible to make a good contact to the Au surface without any damage to the Si diaphragm. This made it possible to measure the specific resistance of the fragile sample. Fig. 9(c) shows the specific measurement results for the Au thin film deposited onto the Si diaphragm. The experimental results indicated that the measured specific resistances of Au were consistent regardless of whether a flat surface or flexible Si diaphragm is used. Therefore, the proposed S4PP can be utilized in various fields because it can precisely measure the specific resistance of a sample without damaging the sample even if it is a flexible material, in contrast to the commercial L4PP.

IV. CONCLUSION

In this study, a S4PP integrated with 3D polymer springs and liquid metal was designed and fabricated to measure the specific resistances of surfaces with large-step-heights and flexible materials. Polymer coil springs fabricated for self-adjustment of the probe height were optimized by using the commercial finite analysis program COMSOL. The non-toxic liquid metal was filled in the microchannels to provide an electrical connection between the tungsten probes and an external equipment. The liquid metal also acts as a buffer solution to reduce a mechanical shock when the W probe contacts with a sample. This helps to minimize the damage to a fragile sample. To verify the accuracy and reproducibility of the fabricated S4PP, the specific resistances of various metal samples were measured and these results were compared with that of the commercial L4PP. The fabricated S4PP was also applied to characterize the specific resistances of a thin metal layer deposited onto sample surfaces with step heights of 60 and 90 μm. Furthermore, the specific-resistance measurements of a 100-nm-thick Au film deposited on a thin silicon diaphragm with a flexural rigidity of 3.6×10^{-5} N/m confirmed that the proposed S4PP can measure the specific resistance without damage to the flexible samples.

ACKNOWLEDGMENTS

This work was supported by a National Research Foundation of Korea (NRF) under Grant Nos. 2015R1A2A2A05001-405 and 2015R1A4A1041746 funded by the Korean government (MEST), Korean Health Technology R&D Project (No. H113C1527) through the Ministry of Health & Welfare, and the International Collaborative R&D Program through a KIAT grant funded by the MOTIE (No. N0000894).

[1]T. Bae, S. Lee, and J. Hong, Curr. Appl. Phys. **14**, 528–532 (2014).
[2]A. Yoomin, O. Takahito, and E. Masayoshi, J. Micromech. Microeng. **15**, 1224 (2005).
[3]M. C. Benjamin, R. J. Hillard, and J. O. Borland, Nucl. Instrum. Methods Phys. Res., Sect. B **237**, 351–355 (2005).
[4]J. C. Li, Y. Wang, and D. C. Ba, Phys. Procedia **32**, 347–355 (2012).
[5]J.-K. Kim, Y. Zhang, and D. W. Lee, IEEE 22nd Int. Conf. Proc. MEMS 2009 **84-87**, 25–29 (2009).
[6]J.-K. Kim, Y. Zhang, and D.-W. Lee, Rev. Sci. Instrum. **80**, 045107 (2009).
[7]F. Pang, X. Liang, and D. Chen, Rev. Sci. Instrum. **84**, 076104 (2013).
[8]Y. Zhang, J.-K. Kim, C.-S. Park, and D.-W. Lee, Sens. Actuators, A **166**, 247–250 (2011).
[9]T. Kanagawa, R. Hobara, I. Matsuda, T. Tanikawa, A. Natori, and S. Hasegawa, Phys. Rev. Lett. **91**, 036805 (2003).
[10]I. Kazani, G. De Mey, C. Hertleer, J. Banaszczyk, A. Schwarz, G. Guxho, and L. Van Langenhove, Text. Res. J. **83**, 1587–1593 (2013).
[11]Y. Ju, B.-F. Ju, and M. Saka, Rev. Sci. Instrum. **76**, 086101 (2005).
[12]C. L. Petersen, T. M. Hansen, P. Bøggild, A. Boisen, O. Hansen, T. Hassenkam, and F. Grey Sens, Actuators A **96**, 53–58 (2002).
[13]S. Keller, S. Mouaziz, G. Boero, and J. Brugger, Rev. Sci. Instrum. **76**, 125102 (2005).
[14]Y. Kitaoka, T. Tono, S. Yoshimoto, T. Hirahara, S. Hasegawa, and T. Ohba, Appl. Phys. Lett. **95**, 052110 (2009).
[15]C. M. Polley, W. R. Clarke, J. A. Miwa, G. Scappucci, J. W. Wells, D. L. Jaeger, M. R. Bischof, R. F. Reidy, B. P. Gorman, and M. Simmons, ACS Nano **7**, 5499–5505 (2013).
[16]B. F. Ju, Y. L. Chen, and Y. Ge, Rev. Sci. Instrum. **82**, 013707 (2011).
[17]E. L. Silva, R. F. Silva, M. Zheludkevich, and F. J. Oliveira, Rev. Sci. Instrum. **85**, 095109 (2014).
[18]R. Hobara, S. Yoshimoto, S. Hasegawa, and K. Sakamoto, e-J. Surf. Sci. Nanotechnol. **5**, 94–98 (2007).
[19]C. S. Park and D. W. Lee, J. Nanosci. Nanotechnol. **10**, 4955–4959 (2010).
[20]R. Kinder, M. Mikolášek, D. Donoval, J. Kováč, and M. Tlaczala, J. Electr. Eng. **64**, 106–111 (2013).
[21]L. J. van der Pawn, Philips Res. Repts. **13**, 1–9 (1958).
[22]D. K. Schroder, *Semiconductor Material and Device Characterization* (Jonh Wiley&Sons, Inc., Hoboken, New Jersey, 2006).
[23]S. B. Catalano, IEEE Trans. Electron Devices **10**, 185–188 (1963).
[24]L. B. Valdes, Proc. IRE **42**, 420–427 (1954).